Elastic scattering of electrons and positrons from ground ($1\,^1S$) and metastable ($2\,^{1,3}S$) states of helium: A model-potential approach

Indira Khurana, Rajesh Srivastava, and A. N. Tripathi
Department of Physics, University of Roorkee, Roorkee 247 667, Uttar Pradesh, India
(Received 13 April 1987; revised manuscript received 30 December 1987)

A study of elastic scattering of electrons and positrons by helium in its ground as well as its metastable states has been done using a model-potential approach. Reliable static, polarization, and exchange potentials are used to describe the scattering process. Elastic differential and total cross sections are obtained in a wide range of incident projectile energy, viz., from nearly very low energy to 1000 eV. Our results are compared with available experimental data and other theoretical results.

I. INTRODUCTION

There are a fairly large number of theoretical calculations (see Refs. 1–8, and references therein) for the elastic scattering of electrons from the helium atom in its ground state, using various theoretical approaches, because this is the most fundamental process in atomic physics. Out of various studies, the optical-potential model calculations[5,8–10] have proved to be quite useful and a great success in the recent past in general to describe electron-atom elastic scattering. In this model, the effort is directed towards obtaining an equivalent local central potential to approximate the nonlocal potential which arises in the perturbation expansions of the scattering amplitude. Physical effects, such as atomic polarization caused by the incident electron, and exchange distortion of the incident electron, are approximated by the equivalent central potential. The various efforts made were therefore to construct appropriate various polarization and exchange potentials. While considerable effort has been devoted to studying the elastic scattering from the ground state of helium, relatively little attention has been focused in the past on studying the equally important process of elastic scattering of electrons from the metastable ($2\,^1S, 2\,^3S$) states of helium (see, for example, Ref. 11). Study of these excited states is becoming of increasing interest in two ways: firstly, by the collisional cross-section data for such reactions, which are needed in many astrophysical and plasma applications, and secondly, because of the new experimental techniques by which the long-lived metastable states can be easily probed. Theoretically, whatever studies have been made on the elastic scattering of electrons from helium in these excited states, they have produced largely different results from each other. It would therefore be desirable to reassess the situation, particularly with a method (such as the optical-potential approach) which proved quite successful for the e-He ($1\,^1S$) elastic scattering process.

Unlike the study of e^--atom scattering, where a lot of attempts have been made theoretically and experimentally for the last several decades, not much attention[5,8,12,13] has been given to probing a complementary e^+-atom process. However, this situation in the past few years has changed and brought some interesting results for e^+-atom scattering. In fact, if we consider the positron (e^+) as a complementary probe to the electron (e^-), the combination of intriguing differences (opposite sign of the projectile charge and absence of the exchange interaction in the case of the e^+) and, otherwise, similarities to the electron (in mass, charge, and spin), has stimulated numerous experimental and theoretical investigations of e^+-atom collisions since the development of the first practical low-energy e^+-beam scattering experiment in 1972. It is found that, in a number of ways, e^+-gas scattering experiments have been following a path similar to that followed by early e^--gas scattering experiments. In recent years, with the improvement of e^+-beam technology, it is now becoming possible to measure the differential and total cross section for several individual processes. The situation naturally demanded similar development in the theoretical side, and now there are available a few recent reviews of the theoretical aspects of positron-atom scattering (Refs. 13 and 14, and references therein). According to these reviews, the interactions that characterize elastic-atom positron collisions are static, and polarization and the collisions can therefore also be well described in optical-model-potential calculation.

Now if we look back on all the earlier optical-model-potential calculations as applied to elastic e-He ($1\,^1S$) collisions we find that no effort has been made to improve the calculation by adopting an accurate description of the static potential though better polarization potentials were tried, to improve upon the results. In this paper, therefore, we aim to improve the calculations for the elastic e-He ($1\,^1S$) collision by using an improved optical-potential model in which the static potential shall be obtained using a many-parameter (53-term) correlated wave function which also subsequently shall improve the exchange potential (see Sec. II). In addition, the different polarization potential of tested reliability will also be incorporated in the optical potential. We further aim in the present paper to extend similar calculations to the elastic scattering of electrons from metastable ($2\,^{1,3}S$) states of the helium atom in the spirit of applying the optical-potential model to such collisions also. In addition, in view of recent progress in positron-impact studies, both of these two sets of calculations mentioned earlier for $1\,^1S$ and

$2\,^{1,3}S$ states by the electron impact case are extended for positron impact also.

II. THEORY

In the optical-potential method, the Schrödinger equation describing the incident particle (electron or positron) with the helium atom is given by (atomic units are used throughout)

$$[\tfrac{1}{2}\nabla^2+E-V_{\rm opt}(r)]\psi(r)=0\ , \tag{1}$$

where $E=\frac{1}{2}k^2$ is the incident energy of the projectile electron (or positron), $V_{\rm opt}(r)$ is the optical potential of the system whose exact evaluation has not yet been possible, and an approximation is used. In the present investigation, we represent it by a spherically symmetric, localized and real potential so that we can solve Eq. (1) using the partial-wave method. The optical potential consists of static, exchange (which is absent for positron scattering), and polarization potentials expressed as

$$V_{\rm opt}(r)=V_{\rm stat}(r)+V_{\rm pol}(r)+V_{\rm ex}(r)\ . \tag{2}$$

A. Static potential

In Eq. (2), $V_{\rm stat}(r)$ is the static potential (of the target when it is in its nth state, say, ϕ_n) as seen by a projectile (electron or positron) and is written as

$$V_{\rm stat}(r)=\langle\phi_n(\mathbf{r}_1,\mathbf{r}_2)\,|\,V(\mathbf{r}_1,\mathbf{r}_2,\mathbf{r})\,|\,\phi_n(\mathbf{r}_1,\mathbf{r}_2)\rangle\ , \tag{3}$$

with V being represented as the interaction potential between the projectile electron (positron) and the helium target (with two bound electrons having position vectors $\mathbf{r}_1$ and $\mathbf{r}_2$ with respect to the nucleus of the target) and is given by

$$V=\frac{2Z'}{r}-\sum_{i=1}^{2}\frac{Z'}{|\mathbf{r}-\mathbf{r}_i|}\ . \tag{4}$$

Here $Z'=-1$ for electrons and $+1$ for positrons. For $\phi_n(\mathbf{r}_1,\mathbf{r}_2)$ we have used the Hartree-Fock (HF) wave function[15,16] to represent the $1\,^1S$ and $2\,^{1,3}S$ states as well as the accurate many-parameter (53-term) correlated (MPC) wave function due to Weiss[17] for $1\,^1S$ and $2\,^1S$ states. To simplify the expression [Eq. (3)] with the use of MPC wave functions we first put the expression in the following form where the Fourier transform of interaction potential is first taken, viz.,

$$V_{\rm stat}(r)=\frac{2Z'}{r}-Z'\int\frac{d\mathbf{q}}{q^2}e^{-i\mathbf{q}\cdot\mathbf{r}}F_{nn}(\mathbf{q})\ , \tag{5}$$

where the form factor is given by

$$F_{nn}(\mathbf{q})=\sum_{j=1}^{2}\int\int\phi_n^{*}e^{i\mathbf{q}\cdot\mathbf{r}_j}\phi_n\,d\mathbf{r}_1\,d\mathbf{r}_2\ . \tag{6}$$

This form factor is obtained by choosing ϕ_n, the properly orthonormalized MPC wave function,[18] and then bringing the resulting expression for $F_{nn}(q)$ to the following form by utilizing the fitting procedure (see Ref. 18):

$$F_{1\,^1S\text{-}1\,^1S}(q)=\sum_{i=1}^{3}\frac{a_i}{(q^2+\alpha_i^2)^2}+\sum_{i=4}^{5}\frac{a_iq^2}{(q^2+\alpha_i^2)^3}+\sum_{i=6}^{7}\frac{a_iq^4}{(q^2+\alpha_i^2)^4} \tag{7}$$

and

$$F_{2\,^1S\text{-}2\,^1S}(q)=\sum_{i=1}^{3}\frac{a_i}{(q^2+\alpha_i^2)^2}+\sum_{i=4}^{6}\frac{a_iq^2}{(q^2+\alpha_i^2)^3}+\sum_{i=7}^{9}\frac{a_iq^4}{(q^2+\alpha_i^2)^4}\ , \tag{8}$$

where a_i's and α_i's are compiled in Table I. Using these expressions [Eqs. (7) and (8)] for $F_{nn}(q)$, the closed-form expression for $V_{\rm stat}(r)$ [viz., Eq. (5)] is obtained using the following integral:

$$\int\frac{e^{-i\mathbf{q}\cdot\mathbf{r}}}{q^2(q^2+\alpha_i^2)}d\mathbf{q}=\frac{2\pi^2}{r\alpha_i^2}(1-e^{-\alpha_ir})\ . \tag{9}$$

B. Exchange potential

In Eq. (2), $V_{\rm ex}(r)$ is the exchange potential. In general, it is nonlocal but it is converted for the sake of simplicity into the following widely adopted successful equivalent local-energy-dependent exchange potential by Furness and McCarthy[19] and Vanderpoorten:[20]

TABLE I. The expansion parameters of the transition integral $F_{if}(q)$ for $1\,^1S$-$1\,^1S$ and $2\,^1S$-$2\,^1S$ elastic scattering of helium.

	$1\,^1S$-$1\,^1S$		$2\,^1S$-$2\,^1S$	
i	a_i	α_i	a_i	α_i
1	3452.799	4.000 000	125.8359	4.000 000
2	3999.567	2.688 827	0.690 003 5	1.080 629
3	−11 010.02	3.344 414	41.748 42	2.540 315
4	1360.553	2.688 827	81.074 95	4.000 000
5	4364.459	3.344 414	−6.516 982	1.080 629
6	240.2391	2.688 827	−14.978 22	2.540 315
7	−2042.132	3.344 414	−11.534 91	4.000 000
8			3.815 289	1.080 629
9			43.186 21	2.540 315

$$V_{ex}(r)=\tfrac{1}{2}(\tfrac{1}{2}k^2-V_{stat}(r)-\{[\tfrac{1}{2}k^2-V_{stat}(r)]^2+4\pi\rho(r)\}^{1/2}) . \quad (10)$$

Here, $\rho(r)$ is the spherical charge density of the atom. For positron scattering the exchange is absent and hence the V_{ex} term is taken as zero in the calculation.

C. Polarization potentials

The V_{pol} term in Eq. (2) refers to the polarization potential. The polarization is a major type of correlation between incident projectiles (electron or positron) with bound electrons of a target helium atom. $V_{pol}(r)$ is nonlocal but its leading long-range part is $-\alpha_d/2r^4$, where α_d is the static dipole polarizability of the atom. The next most important long-range term, which is due to the static quadrupole polarization and the nonadiabatic and second-order corrections to the static dipole contribution, is of the order of r^{-6}. The short-range behavior is in general not known and has significant diabatic components. Its determination, even approximately for simple atoms, requires a major computational effort. Consequently, many workers have used semiempirical potentials for modeling the polarization effects at short range. One of the simplest and most popular is the asymptotic form multiplied by a short-range cutoff function containing parameters. In essence, the contribution of the r^{-6} term is considered of lesser importance as compared to the dipole term and is expected; the cutoff function represents other contributions. There are various such forms for $V_{pol}(r)$ available and being tested for elastic scattering of electrons from the ground state of helium and mostly the same form is chosen for e^+ scattering. However, we performed our calculations using the following three forms of V_{pol} which are supposed to produce good results for the e-He $(1\,^1S)$ elastic scattering process.

(i) The most widely used polarization potentials for helium in its ground state in previous works were the modified form of the adiabatic polarization potential originally given for hydrogen by Temkin and Lamkin.[21] We choose in the present work one of the following such forms suggested by Khare and Moiseiwitsch:[22]

$$V_{pol}(r)=-\frac{\alpha_d}{2r^4}[1-(1+2y+2y^2+\tfrac{4}{3}y^3+\tfrac{2}{3}y^4+\tfrac{4}{27}y^5)\times\exp(-2y)] , \quad (11)$$

where $\alpha_d(=1.383a_0^3)$ is the dipole polarizability of the helium atom and $y=Z_1r$ with Z_1 is the cutoff parameter equal to 1.4558 which is the same as the variationally determined parameter in the ground-state Hartee-Fock wave function.[15]

(ii) Recently Nakanishi and Schrader[8] through their detailed study on polarization potentials suggested the following potential to be more appropriate than any others previously used:

$$V_{pol}(r)=-\frac{\alpha_d}{2r^4}\omega\left[\frac{r}{\rho}\right] , \quad (12)$$

with the following cutoff function ω defined as

$$\omega(\xi)=(1-e_n^{\xi}e^{-\xi})^m \quad (m=2,\ n=8) .$$

e_n^{ξ} is the following power series for the exponential function, truncated after the nth power of ξ:

$$e_n^{\xi}=\sum_{i=0}^{n}\frac{\xi^i}{i!} .$$

ρ is an adjustable parameter which is related to the effective target radius r_0 as given by $r_0=10.617\rho$ (see Ref. 8). They have selected r_0 in such a way as to give values of scattering length comparable to the accurate results for e^--He or e^+-He elastic scattering. The values of r_0 for e^--He and e^+-He scattering were, respectively, 2.332 and 1.424.

(iii) Finally, we have taken the following energy-dependent and spherically-symmetric-type expression suggested by Onda and Truhlar[23] for $V_{pol}(r)$ which is based on an r^{-6} nonadiabatic correction to the adiabatic polarization potential,

$$V_{pol}(r)=\frac{\alpha_d}{2r^4}(1+6k^2/\bar{\omega}^2r^2)^{-1} , \quad (13)$$

with $\bar{\omega}$ as the mean excitation energy (equal to 1.2 Ry).

The polarization potential for electron (positron) elastic scattering from helium in its $2\,^1S$ (or $2\,^3S$) excited states is not readily available and would require a substantial amount of computation. The effect, however, of the polarization potential for these excited states should be significant and cannot be ignored since the dipole polarizability of the $2\,^1S$ and $2\,^3S$ states (for example) is approximately $802a_0^3$ and $310a_0^3$, which is large compared with the value $1.383a_0^3$ for $1s^2\,^1S$ state. Recently, Parcell *et al.*[24] reported polarization potential data for scattering from the $2\,^1S$ state of helium using a scaling procedure to the Dalgarno-Lynn potential which was originally proposed for scattering from hydrogen and contains all multipoles. These authors[24] have chosen the scaling parameter in such a way that at least the dipole part of the potential has the correct polarizability in the asymptotic region. The following is the fit we obtained to their data for polarization potential:

$$V_{pol}(r)=-\frac{9}{4[(\beta r)^2+d^2]^2}(1+e^{-\beta r}) , \quad (14)$$

where

$$\beta=0.2737 \text{ and } d^2=2.9 .$$

In our calculation, for e^- and e^+ scattering for $2\,^1S$ states, the same above [viz., as given by Eq. (14)] polarization potential has been used. Parcell *et al.*[24] while discussing their above-mentioned polarization potential for the $2\,^1S$ state in their paper also mentioned and compared this polarization potential with that obtained from $2\,^1S$ from a simpler model potential used by Schrader[25] originally for elastic scattering of positrons from a number of atoms. They found a reasonable agreement in the results obtained from both the different polarization potentials. In fact, the potential used by Schrader[25] was of the form $-\alpha_d/2r^4$ for $r>r_0$, and $-\alpha_d/2r_0^4$ for $r\le r_0$, where α_d is the usual dipole polarizability and r_0 is a parameter given by a formula heuristically derived by Schrader[25] and depending on the ionization potential of the atomic state. Due to nonavailability of any other, more suitable, polarization potentials for $2\,^1S$ and $2\,^3S$ states, we choose in this paper therefore for the $2\,^3S$ state the polarization potential as suggested by Schrader[25] and adopt $\alpha_d = 310a_0^3$ and $r_0 = 3.767$. The same polarization potential is also used for both electron and positron impact cases.

After we have obtained a suitable choice of $V_{\rm opt}$ (for each process) as given by Eq. (2), we substitute it in Eq. (1) and use partial-wave expansion for $\psi(r)$ to get

$$\left[\frac{d^2}{dr^2}+k^2-2V_{\rm opt}(r)-\frac{l(l+1)}{r^2}\right]f_l(r)=0 , \qquad (15)$$

where $f_l(r)$ is solved so that it represents the radially scattered asymptotic wave function expressed as

$$f_l(r)\sim\frac{1}{k}\sin(kr-l\pi/2+\delta_l) \quad \text{as } r\rightarrow\infty ,$$

which gives δ_l the phase shift corresponding to the lth partial wave and consequently the following scattering amplitude through which the differential and total cross sections are obtained in conventional manner:

$$f(\theta)=\frac{1}{k}\sum_{l=0}^{\infty}(2l+1)e^{i\delta_l}\sin\delta_l\,P_l(\cos\theta) . \qquad (16)$$

III. RESULTS AND DISCUSSION

A. Electron scattering

Our calculated differential and total cross section results in the entire energy region up to 500 eV compared with the available recent experimental data and other theoretical calculations are displayed in Figs. 1–8. Before we present the details of our results, it is worth mentioning that the differences noticed in our results obtained using the (i) HF and (ii) MPC wave functions are within 8%. Therefore, in order to maintain the clarity of the figures we have plotted in all figures our accurate results obtained through MPC wave functions only.

1. Elastic scattering from $1\,^1S$ state of helium

Results with the various choices of polarization potentials as mentioned earlier in Sec. II [viz., due to Temkin and Lamkin[21,22] (TL), Nakanishi and Schrader[8] (NS), and Onda and Truhlar[23] (OT)] are obtained for the e^--He($1\,^1S$) elastic scattering case. The results obtained by these above-mentioned three different choices due to TL, NS, and OT, are referred to hereafter as P_1, P_2, and P_3, respectively. In addition, as used by many previous workers, another set of calculations (which shall be referred to as P_1') is also performed by taking $y = Z_1 r$ with $Z_1 = 1.3414r$ in Eq. (11) for the polarization potential. This choice of potential for polarization is based on the simple scaling of the TL potential[21] for helium from the hydrogenic potential such that exact asymptotic dipole behavior for He is obtained. Although we shall see further, upon comparison with the figures, that P_1 and P_1' are not much different.

a. Differential cross section (DCS). Figure 1 shows our DCS results (P_1, P_2, and P_3) at an incident electron energy of 18 eV, where largely other data are available, in a wide angular range (0°–180°). Present results are compared with the experimental data of Register *et al.*,[26] Newell *et al.*[27] (available at 17.5 eV), and those of Andrick and Bitsch[28] (at 19 eV) together with the recent theoretical calculation of McEachran and Stauffer[4] (MS) and the R-matrix calculation of Fon *et al.*[3] (FC). Inspection of this figure suggests that in the forward direction, our DCS results, viz., P_1, P_2, and P_3, are quite different from each other. Result P_1 is larger by 15% or more as compared to P_2, while P_3 is smaller than P_2 by almost the same magnitude. The differences among these results narrow down with the increase in scattering angle to an extent that P_2 and P_3 merge with each other at large angles ($\theta > 120°$) but P_1 remains higher by 10% in this angular region. It is noted that P_2 results compare well with the measured data of Register *et al.*[26] and Andrick and Bitsch[28] below scattering angle $\theta < 40°$, while P_3 favors the measurements of Newell *et al.*[27] In the angular region $40° \leq \theta \leq 120°$, all the measurements agree among themselves as well as reasonably well with the present calculations (P_1, P_2, and P_3). Beyond $\theta > 120°$, P_2 and P_3, which have nearly the same magnitude, favor the data of Andrick and Bitsch,[28] whereas P_1 compares better with the data of Register *et al.*[26] and Newell *et al.*[27] Further, below 10°, results of MS[4] overestimate considerably the theoretical (P_1, P_2, P_3, and FC) and experimental results, but above these angles their results lie in-between P_1 and P_2 up to scattering angle $\theta < 30°$ and thereafter merge with P_2. Similarly, R-matrix results (FC) lie between P_1 and P_2 for $\theta < 10°$, while between 10 and 30°, these results fall between P_2 and P_3, and above that show a good agreement with our P_3 result except at large angles $\theta > 120°$ where these results lie between P_1 and P_2.

Figure 2 shows our results at 30 and 40 eV, respectively. In addition, we have also plotted the theoretical results of Scott and Taylor,[29] LaBahn and Callaway,[30] and experimental measurements of McConkey and Preston[31] (available at 31.1 eV). The pattern of variation of DCS is similar to that at 18 eV. It is noticed that the P_1 results and the results of MS agree well in the entire angular region, except in the forward direction. This difference in the forward direction between our P_1 and the MS results may be said to be due to the different choices of the exchange potentials. In the present calculation a local semiclassical exchange (SCE) potential is taken, while MS have treated the exchange nonlocally. The experimental data due to Register *et al.*[26] differ considerably from the data of McConkey and Preston[31] in the entire angular region. Our P_2 results favor the measured value of Register *et al.* in the forward direction but overestimate it in the angular region from 40° to 120° as compared to theirs. On the other hand, McConkey and Preston's data agree well with the P_2 result in this angular region. Similarly, our P_3 results show good agreement with the data of

McConkey and Preston in the forward direction and overestimate in the intermediate-angular region. However, our P_3 results favor very well the measured data of Register *et al.* in this intermediate-angular region. At large scattering angles ($\theta > 120°$), the behavior is exactly the same as noticed in Fig. 1. The other theoretical calculations, such as the R-matrix results and the second-order potential calculations of Scott and Taylor,[29] compare well with the P_2 result except at low angles. In general, it is found that the general shape of the experimental measurements is well reproduced by the present (P_1, P_2, and P_3) as well as other theoretical calculations including the location of the minimum of cross section.

Figure 3 shows our present results (P_1, P_2, and P_3) for DCS along with various theoretical calculations[7,11,15,29] and experimental[2,26,32,33] results at 100 and 200 eV, respectively. The DCS shows a dominant forward scattering behavior without a minimum as noticed at energies below 50 eV. All the experimental results have similar shape but differ in magnitude. It is seen that our P_1 and P_2 results have good agreement with all the measurements in the angular region $\theta \leq 40°$. Beyond $\theta > 40°$, the

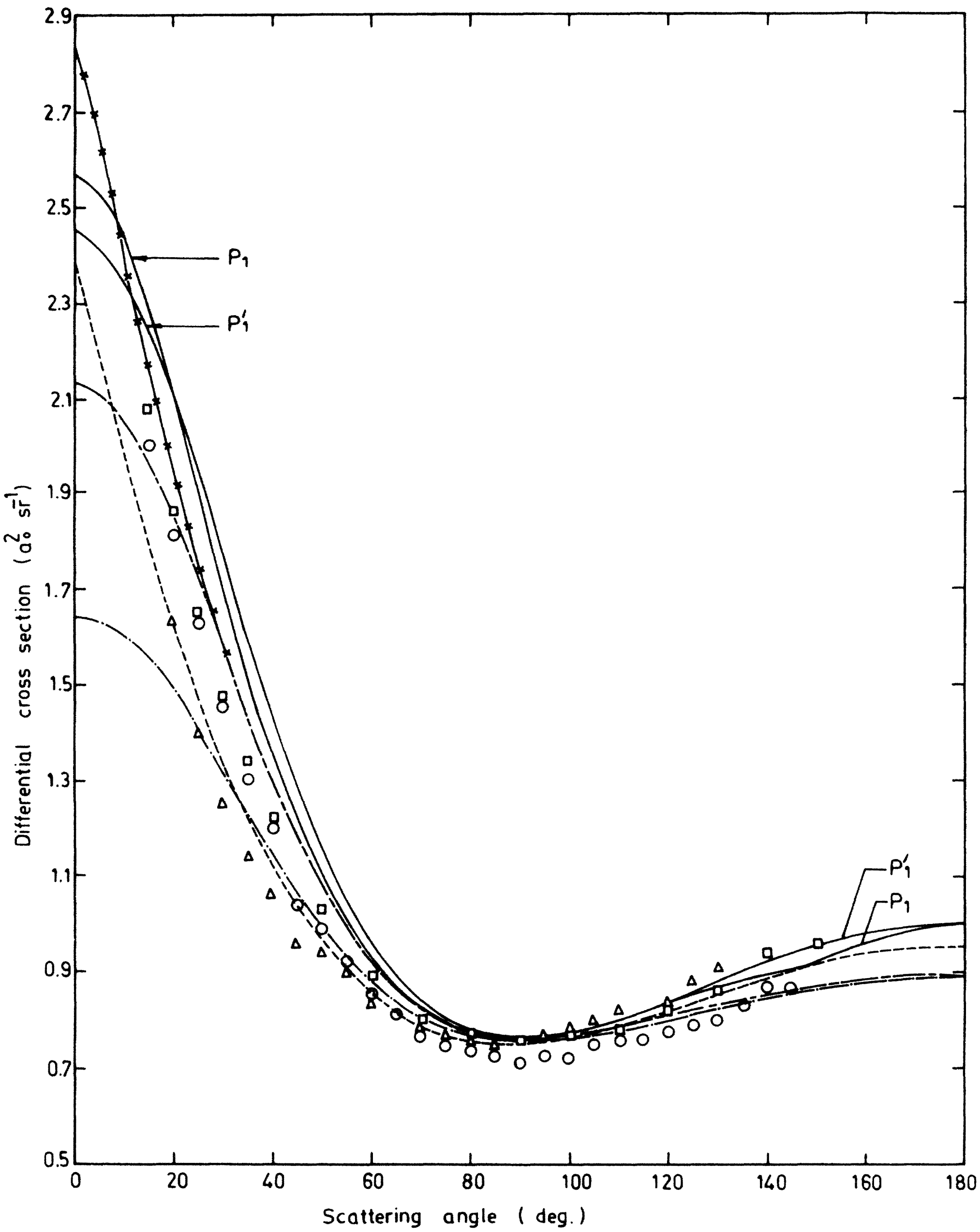

FIG. 1. Differential cross section for elastic e^--He ($1\,^1S$) scattering at 18-eV electron-impact energy. ——, present P_1 and P_1' results (see text); ---, present P_2 results; –·–, present P_3 results; –×–, adiabatic-exchange approximation (Ref. 4); ---, R-matrix calculation (Ref. 3); △, experiment (Ref. 27); □, experiment (Ref. 26); ○, Andrick and Bitsch (Ref. 28).

present results P_1, P_2, and P_3 approach each other and become almost identical. They show a good agreement with the data of Shyn.[2] In the forward direction the P_1 result agrees well with the theoretical calculation of Byron and Joachain[34] obtained using the eikonal Born series (EBS) method, and agrees with recent calculations of Khare and Lata[7] (KL), but differs considerably in the backward direction, where results of KL underestimate all the experimental data, but EBS results are only lower than the experimental data of Shyn. The situation at 200 eV [see Fig. 3(b)] is very similar to the results shown at 100 eV. The different results tend to merge into each other with an increase in scattering angles, except for the results of KL which underestimate the cross section ($60° \leq \theta \leq 160°$). The overall agreement of our results with the experimental data is comparable with that of the EBS and many-body theory[29] (MBT), and is better than that of other theoretical results.

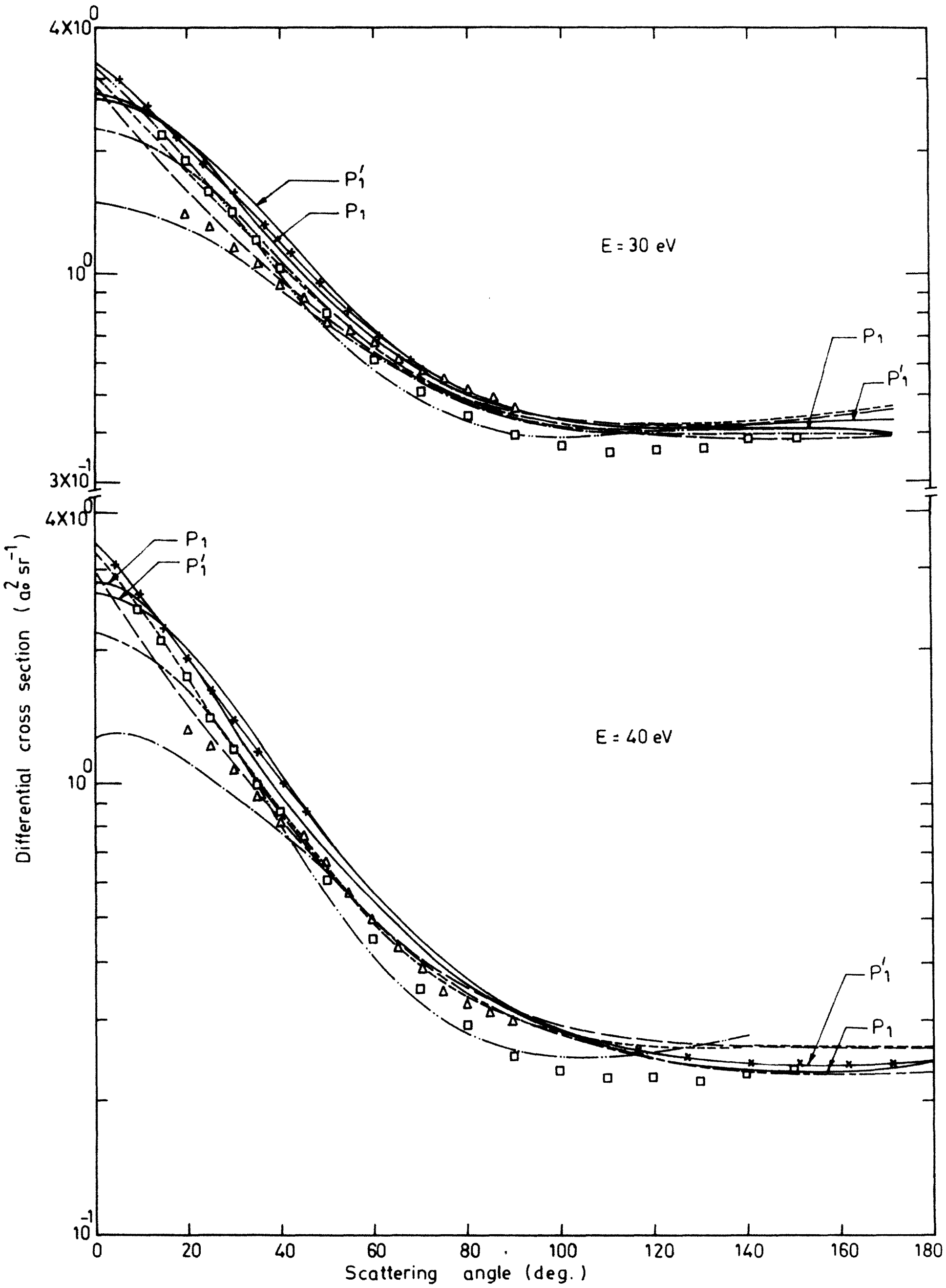

FIG. 2. Differential cross section for elastic e^--He ($1\,^1S$) at 30- and 40-eV electron-impact energy. Same as Fig. 1 except — — —, extended-polarization potential method (Ref. 30); –··–, second-order many-body theory (Ref. 29); △, experiment (Ref. 31).

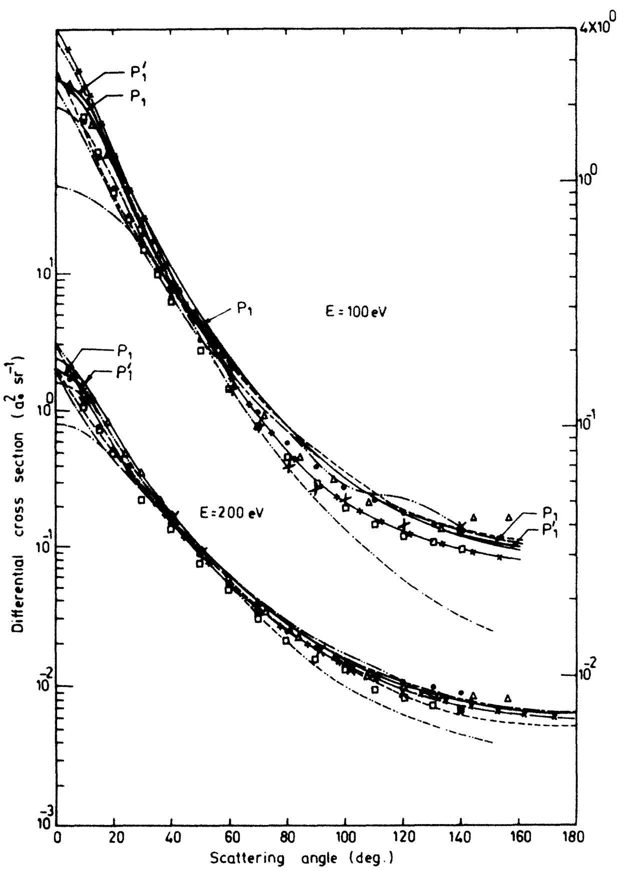

FIG. 3. Differential cross section for elastic e^--He ($1\,^1S$) at 100- and 200-eV electron-impact energy. Same as Fig. 2 except $-\cdots-$, Khare and Lata (Ref. 7); $-\times-$, EBS results (Ref. 34); ●, experiment (Ref. 33); ×, experiment (Ref. 32); △, experiment (Ref. 2). Scale on right-hand side is for the results at 200 eV.

b. Total cross section. Figure 4 displays our total scattering cross-section results for electrons elastically scattered from a helium atom. We have plotted our results in two parts: (i) in a low-energy range up to 20 eV, and (ii) in an intermediate-energy range between 20 and 200 eV. A large number of theoretical and experimental data are available for the total scattering cross section of helium in its ground state, but to maintain the clarity of the figure, we have compared the present results with a few theoretical[4,8,10,11,29,30,35] and experimental[26–28,36–39] results including the recent measurements of Nickel *et al.*[40] From Fig. 4 we see that there is a large discrepancy among the three sets (P_1, P_2, and P_3) of present results in the low-energy region (below 5 eV). This large variation suggests that the present model may not be reliable at such low energies, although one does find that P_1 results agree well with the measured data of Charlton *et al.*[38] and Nickel *et al.*[40] between 2 and 4 eV. Between 5 and 10 eV, the P_2 and P_3 results lie close to each other while P_1 underestimates these results by 5%. Between 10 and 20 eV, P_1 is larger compared to P_2 and P_3, while P_2 falls in-between P_1 and P_3 and show good agreement with the recent measurements of Nickel *et al.*[40] It should be noted that experimental results for the total elastic cross section obtained by Andrick and Bitsch,[28] Newell *et al.*,[27] and Register *et al.*[26] are derived from the analysis of measured DCS values and are not direct measurements. On the other hand, Kennerly and Bonham[37] (KB), Blaauw *et al.*,[36] Charlton *et al.*,[38] and Nickel *et al.*[40] have reported direct measurement for the elastic integral cross section below the first inelastic threshold. It is noticed that in the energy region from 4 to 20 eV, a very good agreement exists between these four sets of direct measurements and the theoretical calculations of Nesbet[35] and LaBahn and Callaway.[30] The difference among these measurements and the present calculations (P_1, P_2, and P_3) varies within 5 to 15%. In the energy region 20–50 eV the present P_2 results show good agreement with the calculations of Fon *et al.*,[11] the many-body theory of Scott and Taylor,[29] the MS[4] calculations, and with the experimental measurements of deHeer and Jansen,[39] Register *et al.*,[26] and Kennerly and Bonham.[37] Beyond 50 eV, the difference between P_1, P_2, and P_3 narrows down and finally P_2 and P_3 coincide with each other at 100 eV. P_1 remains higher than P_2 and P_3 results by about 25% up to 200 eV. Note that the P_1 result merges with P_2 and P_3 at energies well above 400 eV (not shown here, though). In the energy region, (i.e., 100–200 eV), the present results P_2 and P_3 agree reasonably well with the recent measurements of Nickel *et al.*[40]

2. *Electron-helium scattering for $2\,^{1,3}S$ states*

a. Total cross section. The model-potential approach has been used for the first time to study the elastic scattering of helium from the metastable ($2\,^{1,3}S$) states. Apart from the calculations by Bhattacharya[41] and Taylor[42] in the first Born approximation and Chen and Khayrallah[43] in the Glauber approximation at high energies, most of the calculations available in the literature, such as close coupling due to Marriot[44] and Burke *et al.*,[45] extended-polarization approximation by Sklarew and Callaway,[46] variational calculation by Oberoi and Nesbet,[47] polarized core approximation by Hussain *et al.*,[48] effective potential calculation by Robinson,[49] and a five-state R-matrix calculation due to Fon *et al.*,[11] are in the low-energy region. So far only two experiments, due to Wilson and Williams[50] and Neynaber *et al.*,[51] have been carried out to measure the absolute total scattering cross sections of electrons by metastable helium ($2\,^3S$) in the low-energy region (below 10 eV). For the electron elastic scattering from the metastable ($2\,^{1,3}S$) states, we have employed only one type of polarization potential [Eq. (14)] as mentioned in Sec. II. The results are presented in the following four forms of calculations, namely, using model potential (i) only as with static potential (V_{stat}), (ii) with static and polarization potentials, (iii) with static and exchange potentials, and (iv) with static, polarization, and exchange potentials (SPE). It is clearly seen from Fig. 5, for $2\,^1S$ total elastic scattering cross section (σ_T) that the inclusion of the polarization potential enhances the σ_T by a factor of 5 compared to the results obtained by using only the static potential. The inclusion of the exchange potential produces very small changes in the σ_T, as expected at low energies only. In the energy region below 10 eV, the present SPE calculations agree well with results of Hussain *et al.*[48] and *R*-matrix results of Fon *et al.*[11] The close-coupling results of Marriot[44] lie considerably lower than the present results. Beyond 10 eV, the SPE results decrease slowly and tend, as expected, to first Born and Glauber results at very high energy ($\simeq$1000 eV). In contrast, the *R*-matrix results fall off very rapidly and merge to Born results at 100 eV. In Figs. 6(a) and 6(b), for elastic scattering of electrons from the $2\,^3S$ state of helium, the situation is very similar to the case of electron elastic scattering from the $2\,^1S$ state, except that the exchange contribution is relatively large for the case of the $2\,^3S$ state of helium, particularly in the low-energy region (1–10 eV) where shape resonances are dominant. Present SPE calculations for the $2\,^3S$ state [see

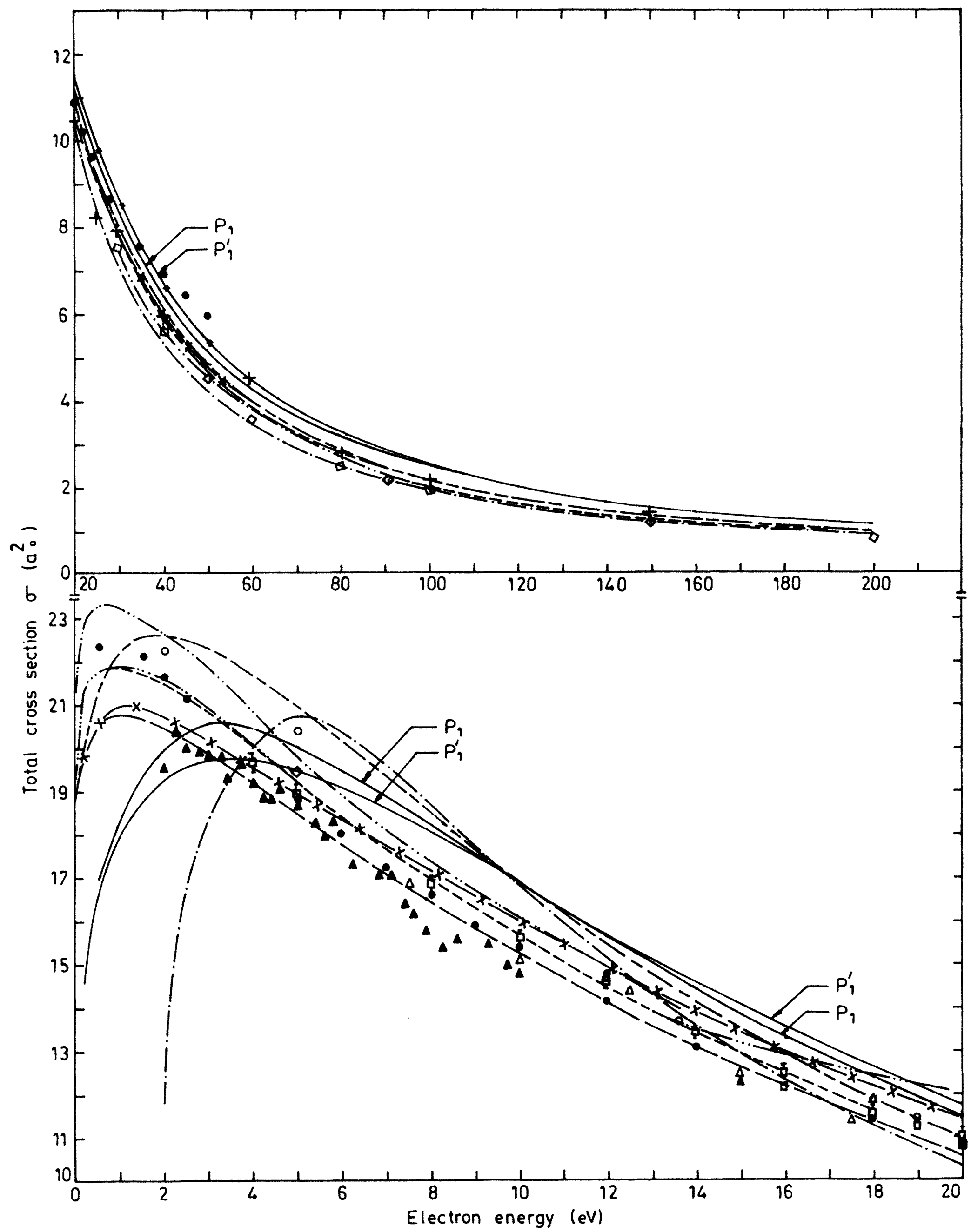

FIG. 4. Total elastic cross section for the e^--He ($1\,^1S$) scattering. Same as Fig. 1 except ---, Nesbet (Ref. 35); –··–, model-potential method results (Ref. 10); –···–, optical-potential model calculation (Ref. 8); ----, *R*-matrix results (Ref. 3); –··–, second-order many-body theory (Ref. 29); — — —, extended-polarization potential method (Ref. 30); ■, experiment (Ref. 36); ●, experiment (Ref. 37); ▲, experiment (Ref. 38); ☐ with error bar, experiment (Ref. 40); ◇, experiment (Ref. 26); +, experiment (Ref. 39).

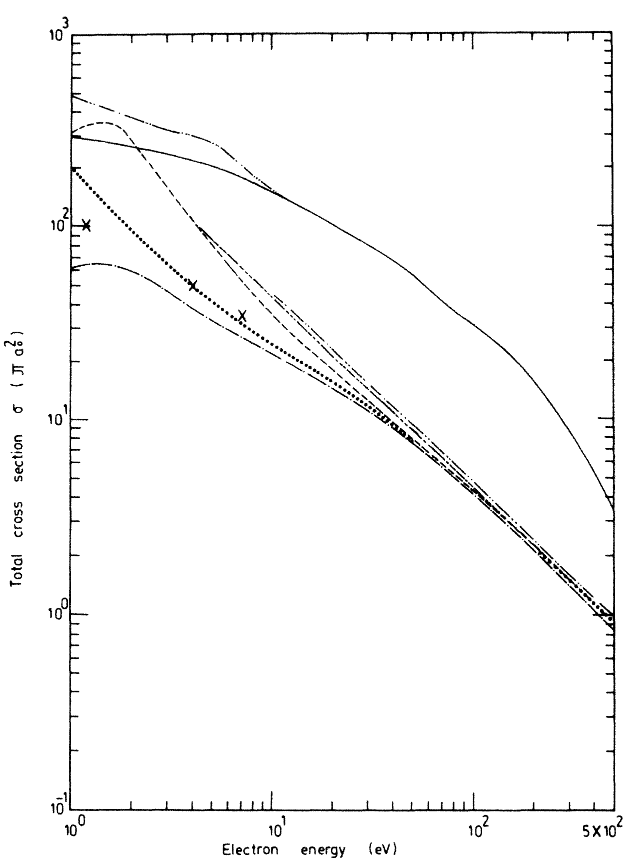

FIG. 5. Total elastic cross section for the e^--He ($2\,^1S$) scattering. —·—, present results with static potential only; ——, present SPE results; -----, first Born results (Ref. 42); —··—, Glauber results (Ref. 43); —···—, Hussain *et al.* (Ref. 48); ---, *R*-matrix results (Ref. 11); ×, close-coupling results (Ref. 44); ..., present results with static and exchange potentials only.

Fig. 6(b)] when compared with the measurements of Neynaber *et al.*,[51] suggest that above 1 eV, the results from measurements are much larger than the present calculations and all the other theoretical elastic scattering cross sections. The theoretical cross sections decrease rapidly with energy while the measured cross sections fall very slowly with energy. It is also seen that the present SPE results throughout the energy range, i.e., 1–10 eV, are larger than those calculated by Sklarew and Callaway[46] in their extended-polarization method as well as in the static approximation, but are smaller than their exchange-adiabatic approximation results and also smaller than the polarized core results of Hussain *et al.*,[48] though both of these results show a better agreement with the experimental data. The resonances seen in the *R*-matrix results of Fon *et al.*[11] may be due to their inclusion of contributions due to the coupling between the $2\,^{1,3}S$ and $2\,^{1,3}P$ states. Otherwise, their results are in harmony with the present calculations only up to 3 eV but thereafter theirs fall off more rapidly and converge to the first Born results at 100 eV. In contrast to this feature, the present calculations show a poor convergence to first Born results and approach the Born results at much higher incident energy ($\simeq$1000 eV not shown here). The enhancement and the slow convergence of the cross section may be related to the large dipole polarizabilities of the metastable states ($802a_0^3$ for $2\,^1S$ and $310a_0^3$ for $2\,^3S$).

b. Differential cross sections. Figures 7 and 8 display our differential scattering cross section SPE results for the elastic scattering of electrons by metastable $2\,^1S$ and $2\,^3S$ states of helium, respectively, in an energy range 50–500 eV. There are no experimental measurements and theoretical calculations available for comparison except the Glauber calculation of Chen and Khayrallah.[43] At intermediate energies (50 and 100 eV), where we expect our model to predict reliable results, the Glauber calculations are found to underestimate considerably (see Figs. 7 and 8). The discrepancy with the Glauber calculation is not surprising as it well known that the conventional Glauber approach may not be reliable as it neglects the intermediate-energy transfer.

B. Positron scattering

1. Positron-helium scattering from ground ($1\,^1S$) state

a. Total cross section. During the last few years, the study of positron-gas scattering with inert atoms has become an active area of research both theoretically and experimentally. Total elastic cross sections have been measured for low-energy positrons colliding with helium by several different experimental groups (Canter *et al.*,[52] Stein *et al.*,[53] and Coleman *et al.*[54]). Very recently, Sinapius *et al.*[55] and Mizogawa *et al.*[56] have measured the total cross sections for positrons colliding with helium in the energy range 0.2–22 eV. These experiments have attracted various theorists to calculate the total cross sections of the e^+-He system in a wide energy range. In view of this, we have also extended our model-potential approach to compute the total elastic scattering cross section for this system in the low- and intermediate-energy range (0.1–200 eV). In our calculations we have not taken into account the contribution arising due to positronium formation. Figure 9 displays our total cross-section results calculated in the previously mentioned three different forms, viz., P_1, P_2, and P_3, analogous to electron scattering as a function of wave numbers of incident positrons. In addition, we have also plotted several theoretical results such as the model-potential calculation of Khan *et al.*,[5] a random-phase-approximation calculation of Amusia *et al.*,[57] the polarized orbital method results of McEachran *et al.*,[58] and the recent results of Nakanishi and Schrader[8] employing a semiclassical potential together with the experimental measurements of Sinapius *et al.*[55] and Mizogawa *et al.*[56] It is clearly seen that the results obtained from various theoretical approaches differ considerably among themselves throughout the energy range. Our P_1 results predict a deep Ramsauer minimum at the lower side of the energy (1.3 eV), whereas the results of Khan *et al.*[5] show this minimum at the higher side of the energy (i.e., 3 eV). The experimental measurement suggests a minimum at 2 eV which agrees well with the predictions of Nakanishi

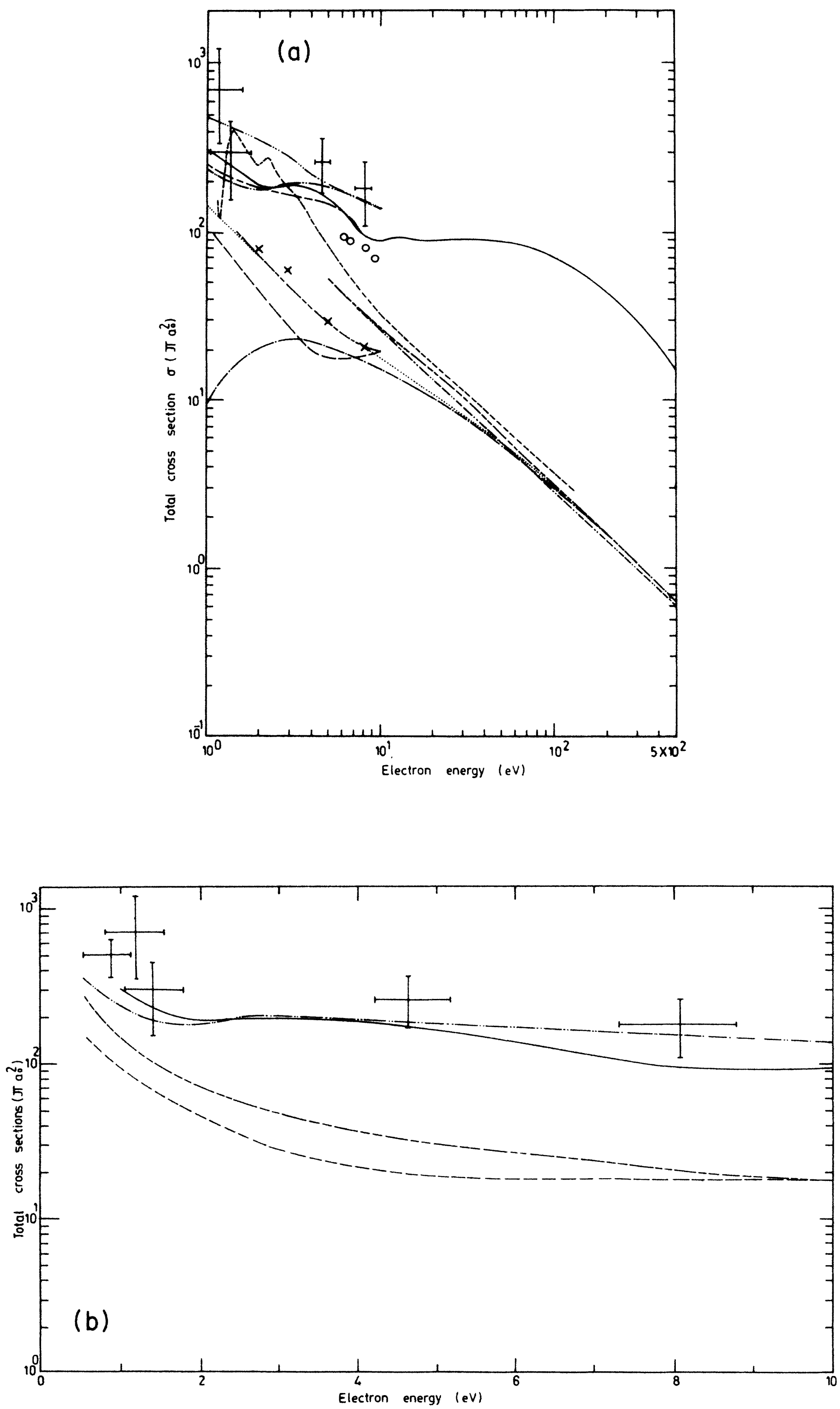

FIG. 6. (a) Total elastic cross section for the e^--He ($2\,^3S$) scattering. Same as Fig. 5 except –·–, present results with static plus polarization potential; –··–, exchange-adiabatic approximation (Ref. 46); ----, static approximation (Ref. 46); — — —, extended-polarization model (Ref. 46); ○, effective potential calculation (Ref. 49); +, experiment (Ref. 51). (b) Total elastic cross section for the e^--He ($2\,^3S$) scattering. Same as (a).

and Schrader.[8] Beyond the Ramsauer minimum, the present P_1 results merge with the result of Nakanishi and Schrader and show a good agreement with the measurement of Mizogawa *et al.*[56] up to 18 eV. In this energy region the result of Khan *et al.*[5] is smaller by about 20% compared to the present P_1 result. The results of Khan *et al.* show a close similarity with the results of McEachran *et al.*[4] in the entire energy region. The sudden rise in the experimental measurements of Mizogawa *et al.* beyond 18 eV is not seen in any theoretical calculations and measurements reported by other groups.

The upper part of Fig. 9 displays our results compared with other theories in the energy region (50–200 eV). It is noticed from this figure that all the present results P_1,

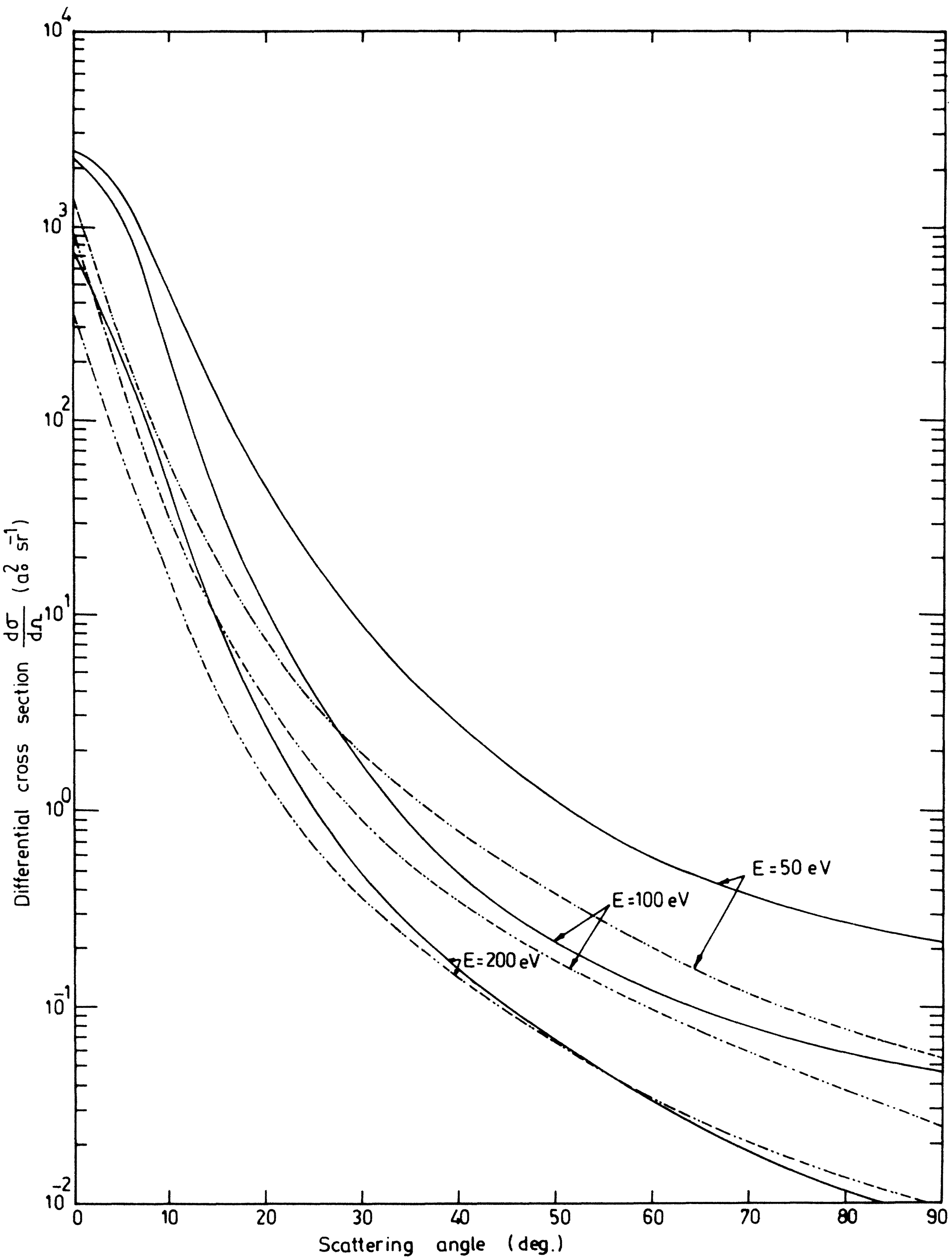

FIG. 7. Differential cross section for elastic e^--He ($2\,^1S$) scattering at 50-, 100-, and 200-eV electron-impact energies. Same as Fig. 5.

P_2, and P_3 differ among themselves as usual in the low-energy region but approach the same value at very high energy ($E_i > 500$ eV). The three-state close-coupling (3CC) results of Willis *et al.*[59] and the second-order potential results of Mukherjee and Sural[60] agree well with our P_3 results. We also see that the results of Byron and Joachain[34] using the optical model are quite close to our P_1 calculations.

b. Differential cross sections. Other theoretical calculations for the differential cross sections for the elastic scattering of positrons by helium from its ground state are available either at very low or at very high energies of

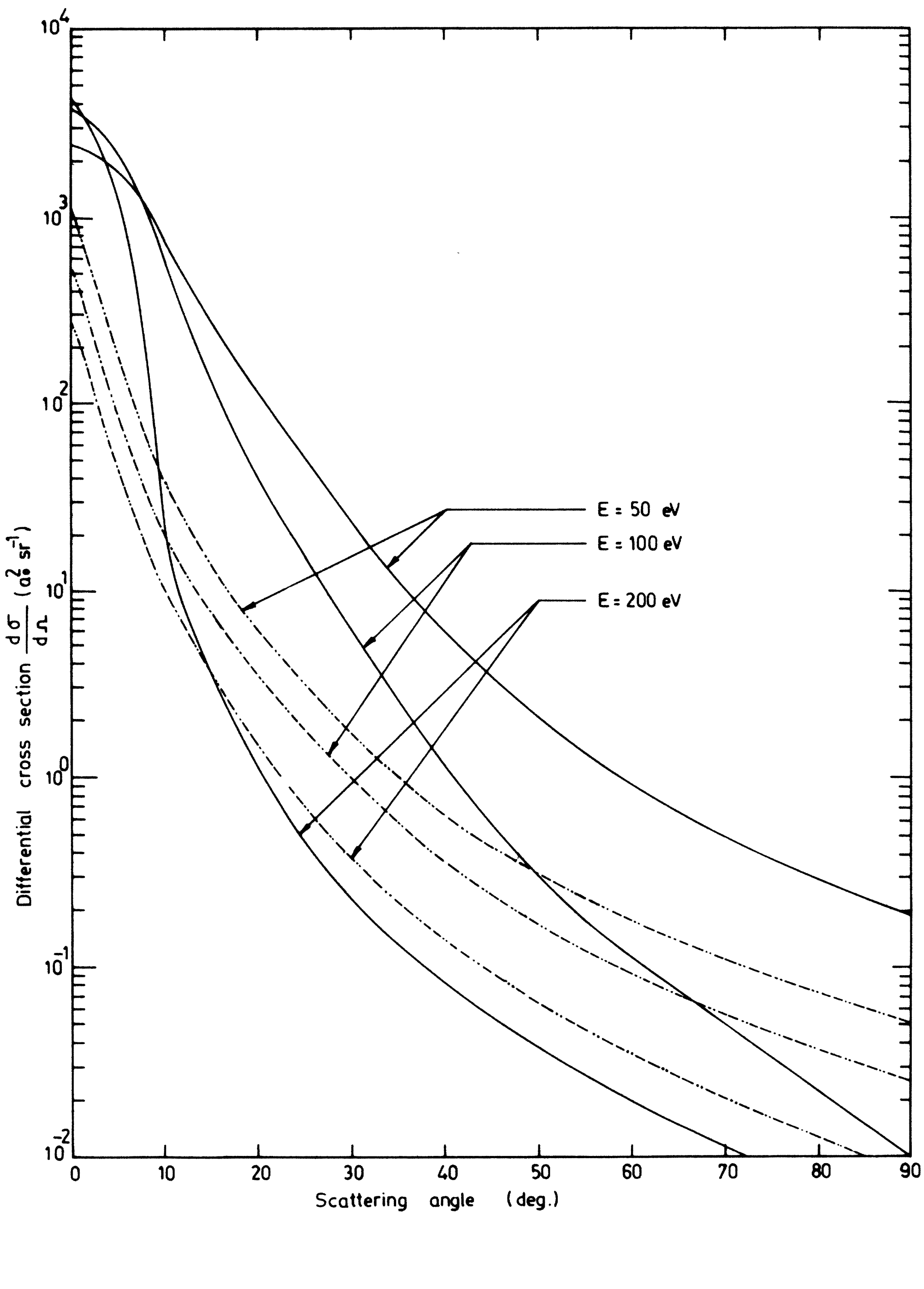

FIG. 8. Differential cross section for elastic e^--He ($2\,^3S$) scattering at 50-, 100-, and 200-eV electron impact energies. Same as Fig. 5.

impact. For the sake of comparison with these available results we display our DCS results along with them at 15 eV and 100 eV in Figs. 10 and 11, respectively. From Fig. 10, which displays our results (P_1, P_2, and P_3) along with the model-potential results of Khan *et al.*[5] at 15 eV, we see that all the results except P_3 show a minimum in the small-angular region ($20° \leq \theta \leq 50°$) which arises due to the interference between the static and polarization potential contributions being opposite in signs. It is noted that this feature has disappeared in the present P_3 results. In the forward direction, the P_2 result lies above P_1, while in the intermediate-angular region, the positions of P_1 and P_2 results are reversed. In the backward direction, all the results, as expected, approach each other. It can be seen that the second maxima of all the curves fall between scattering angles 40° and 80°. The model-potential results of Khan *et al.*[5] overestimate P_1 at small scattering angles while they are in good agreement with P_2 in shape and magnitude. However, at intermediate scattering angles their results underestimate P_1 and overestimate P_2.

Present DCS results at 100-eV positron-impact energy

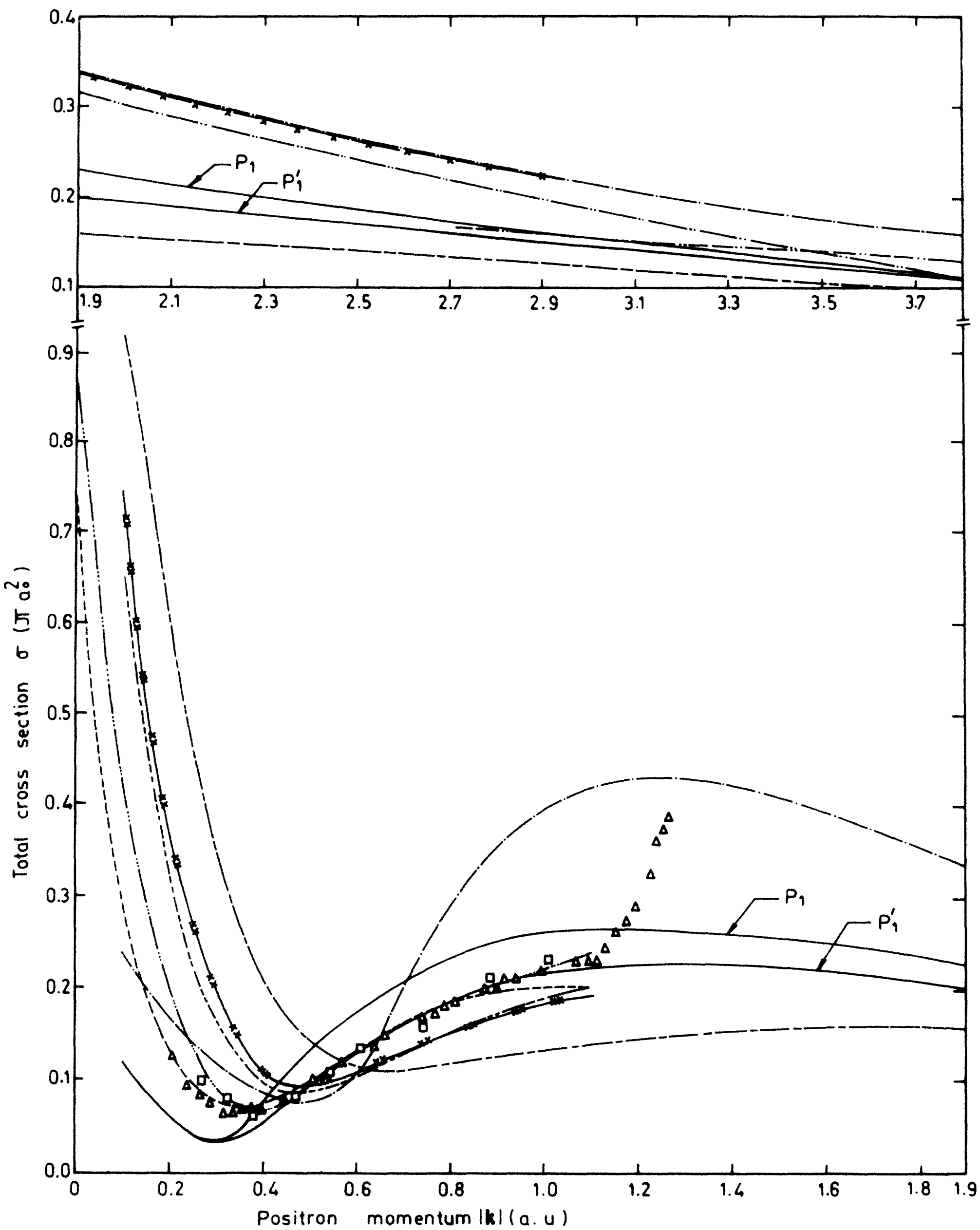

FIG. 9. Total elastic cross section for the e^+-He ($1\,^1S$) scattering. ---, present P_1 results; ---, present P_2 results; – · –, present P_3 results; – × × –, McEachran and Stauffer (Ref. 58); ----, model-potential results (Ref. 5); – ··· –, best values of NS (Ref. 8); ---, Amusia *et al.* (Ref. 57); – ·· –, SOP results (Ref. 60); – × –, 3CC results (Ref. 59); – ·· –, OM results (Ref. 34).

are shown in Fig. 11. We compare our results with the results obtained in the eikonal Born series method of Byron and Joachain,[34] the Coulomb-projected Born polarization (CPBP) approximation due to Gupta and Mathur,[61] and recent calculations by Khare and Lata.[7] From the figure we notice that the situation of the present results P_1 and P_2 is reversed in this case as compared to 15 eV in an angular range (0°–60°). Above 60°, all the present results coincide with each other. The CPBP results show a minimum in the same angular region as P_2. The EBS results and the results of KL lie below the present results, while the optical model (OM) results of Byron and Joachain give the highest DCS's in the entire angular range except 25°–60°.

c. Positron-helium scattering for $2\,^{1,3}S$ *states.* Since no other results have so far been reported for the elastic scattering of metastable helium ($2\,^{1,3}S$) by positron impact, we therefore, for the sake of completeness, present our DCS results at a few incident positron energies in Fig. 12. However, our total cross-section results in the energy range 15–1000 eV are compiled in Table II. It is seen (Fig. 12) that at all the energies, the nature of the curves for DCS is very similar to what we have observed in the case of corresponding electron scattering of helium

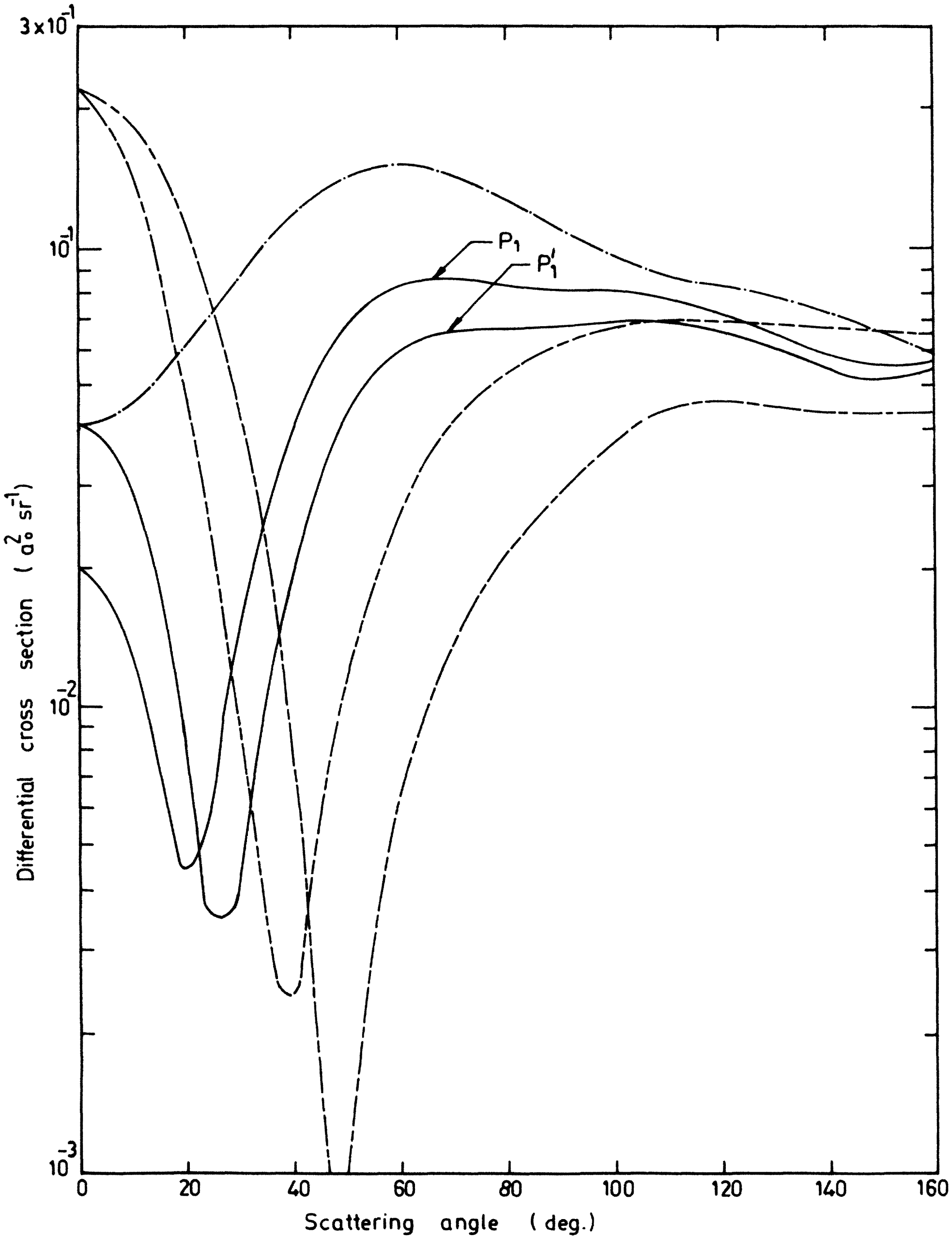

FIG. 10. Differential cross sections for elastic e^+-He ($1\,^1S$) at 15-eV positron-impact energy. Same as Fig. 9.

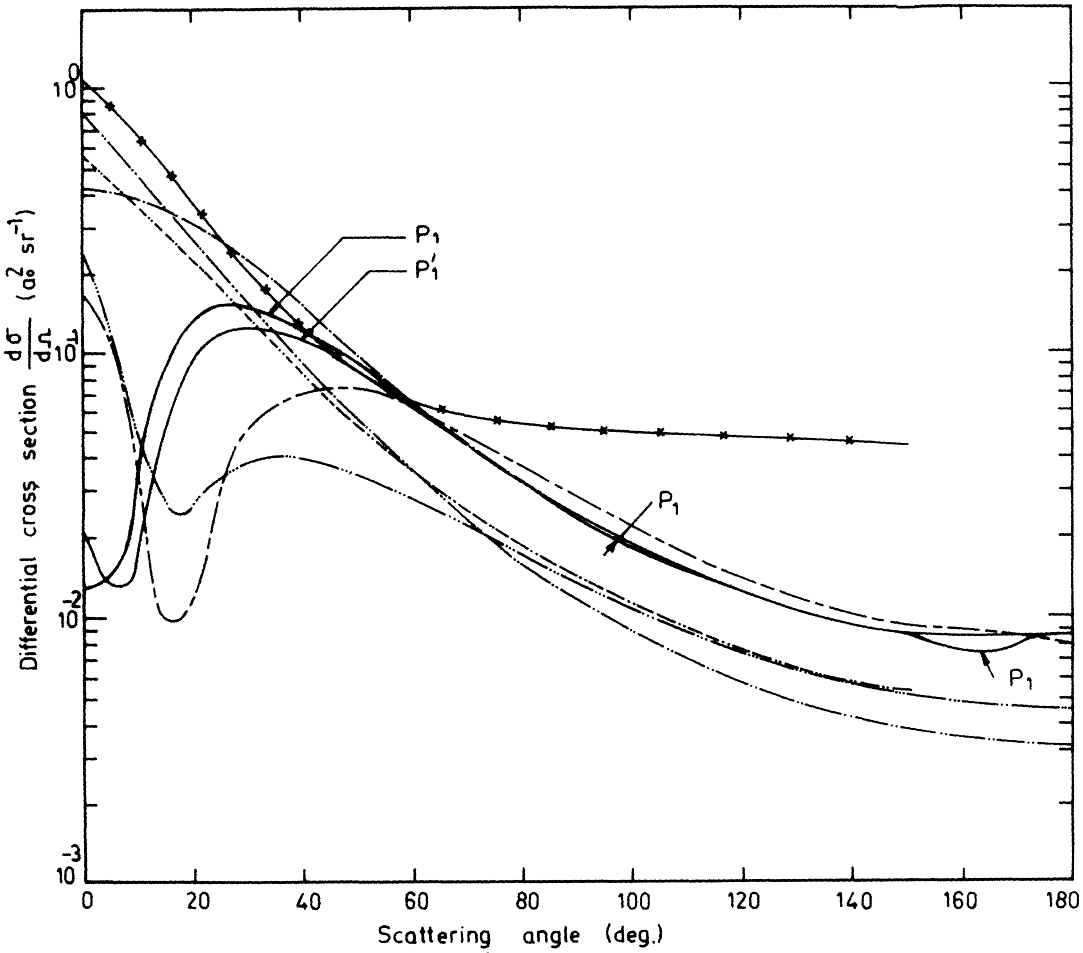

FIG. 11. Differential cross sections for elastic e^+-He ($1\,^1S$) scattering at 100-eV positron-impact energy. Same as Fig. 3 except –×–, OM results (Ref. 34); –··–, EBS results (Ref. 34); –···–, CPBP results (Ref. 61).

TABLE II. Total elastic cross section for e^+-He ($2\,^1S$) and He ($2\,^3S$) scattering in units of (πa_0^2).

Energy (eV)	$2\,^1S$ P_1	$2\,^1S$ P_2	$2\,^3S$ P_1	$2\,^3S$ P_2
1	9.85[−1][a]	2.75[+1]	2.80[−1]	1.79[+1]
2	9.69[−1]	2.48[+1]	2.78[−1]	1.62[+1]
3	9.54[−1]	2.29[+1]	2.76[−1]	1.50[+1]
4	9.39[−1]	2.14[+1]	2.75[−1]	1.40[+1]
5	9.25[−1]	2.01[+1]	2.73[−1]	1.32[+1]
6	9.12[−1]	1.89[+1]	2.72[−1]	1.25[+1]
7	9.00[−1]	1.79[+1]	2.70[−1]	1.18[+1]
8	8.88[−1]	1.70[+1]	2.68[−1]	1.13[+1]
9	8.77[−1]	1.63[+1]	2.67[−1]	1.08[+1]
10	8.66[−1]	1.56[+1]	2.65[−1]	1.03[+1]
20	7.76[−1]	1.11[+1]	2.51[−1]	7.46
30	7.07[−1]	8.73	2.39[−1]	5.92
40	6.49[−1]	7.22	2.29[−1]	4.93
50	6.00[−1]	6.17	2.19[−1]	4.24
60	5.56[−1]	5.40	2.10[−1]	3.73
70	5.17[−1]	4.76	2.02[−1]	3.30
80	4.83[−1]	4.29	1.95[−1]	3.01
90	4.53[−1]	3.91	1.88[−1]	2.73
100	4.26[−1]	3.60	1.81[−1]	2.51
200	2.69[−1]	1.96	1.31[−1]	1.41
500	1.32[−1]	8.54[−1]	6.92[−2]	6.13[−1]
1000	8.50[−2]	4.37[−1]	4.85[−2]	3.42[−1]

[a]Number enclosed in square brackets denotes the power of ten by which the quantity is to be multiplied.

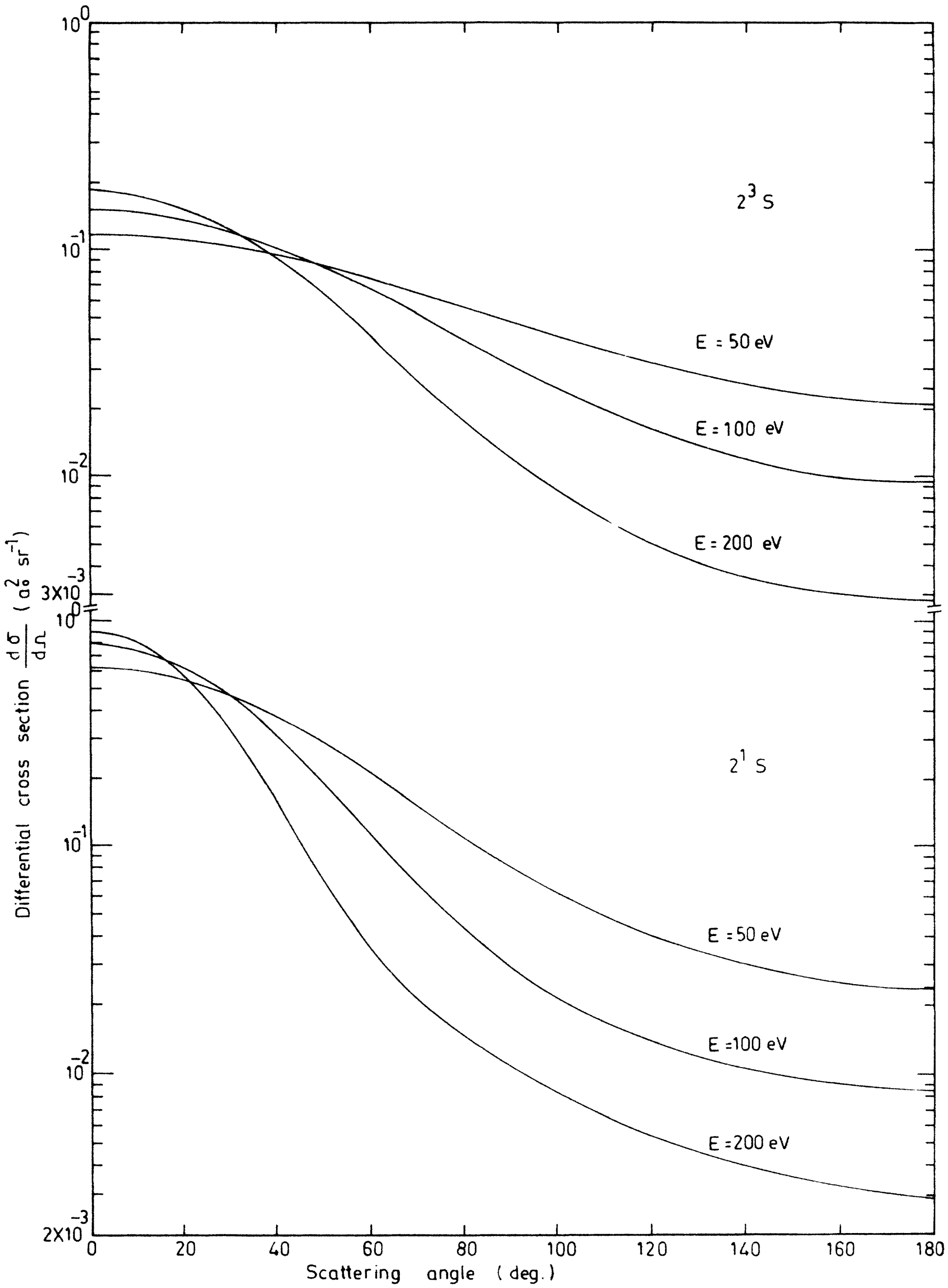

FIG. 12. Differential cross sections for elastic e^+-He ($2\,^1S$) and ($2\,^3S$) scattering at 50-, 100-, and 200-eV positron-impact energies. Same as Fig. 5.

from their metastable states. The rest of our electron- and positron-impact cross-section results, not presented here, are compiled elsewhere[62] and readers can obtain these upon request to us.

IV. CONCLUSION

We have presented the elastic scattering of electrons and positrons from ground ($1\,^1S$) and metastable ($2\,^{1,3}S$) states of helium in a wide energy range (18–500 eV) by using a model-potential approach. One of the important aspects of the present calculation is that the static potential is constructed by using a very accurate many-parameter correlated wave function. The effect of exchange is most accurately represented by a local semiclassical exchange. The polarization is described through the three different forms of the parameter-dependent polarization potential, namely, (i) that of Temkin and Lamkin, (ii) that of Nakanishi and Schrader, and that of (iii) Oda and Truhlar. Further, we wish to add that the polarization potentials as used in the present calculation (at the Hartree-Fock level) cannot be said to be as accurate as our choice of static and exchange potentials.

We finally conclude that for the electron scattering the dipole part of the polarization and semiclassical exchange, together with the accurate static potential representing the full interaction, predicts results in good agreement with the measured values and more elaborate theoretical calculations, in particular at intermediate and high energies. In the low-energy region, the present results (P_1, P_2, and P_3) differ among themselves appreciably and are not fully capable of reproducing the observed experimental features accurately. This clearly indicates that for low-energy electrons ($E \leq 20$ eV) scattering another proper combination for polarization and exchange potentials to probe the inner region of the atomic system might be worth attempting. In this respect the present polarization along with the chosen exchange potential is just not totally adequate to describe the physical nature of the scattering process in the entire energy region. For the positron scattering from the ground state the present combination of static along with the semiempirical form of polarization due to NS is very successful and predicts a reliable total cross section in the entire energy region. Electron elastic scattering from metastable ($2\,^{1,3}S$) states is nicely described by present calculations, except that at the higher-energy region where no experimental results are available as in this region, the polarization effect dominates and shows a large contribution. Nothing can be said for positron scattering results for elastic scattering from metastable ($2\,^{1,3}S$) states until experimental results are made available.

ACKNOWLEDGMENTS

We are thankful to the Council for Scientific and Industrial Research (CSIR), New Delhi, India, for financial assistance received by us in different forms. One of us (R.S.) is also grateful to Professor D. M. Schrader for fruitful discussions with him.

[1]J. Callaway, Adv. Phys. **29**, 771 (1980).
[2]T. W. Shyn, Phys. Rev. A **22**, 916 (1980).
[3]W. C. Fon, K. A. Berrington, and A. Hibbert, J. Phys. B **14**, 307 (1981).
[4]R. P. McEachran and A. D. Stauffer, J. Phys. B **16**, 255 (1983).
[5]P. Khan, S. K. Datta, D. Bhattacharya, and A. S. Ghosh, Phys. Rev. A **29**, 3129 (1984).
[6]H. R. J. Walters, Phys. Rep. **116**, 1 (1984).
[7]S. P. Khare and K. Lata, J. Phys. B **18**, 2941 (1985).
[8]H. Nakanishi and D. M. Schrader, Phys. Rev. A **34**, 1810 (1986).
[9]M. R. C. McDowell, Comments At. Mol. Phys. **9**, 127 (1980).
[10]J. K. O'Connell and N. F. Lane, Phys. Rev. A **27**, 1893 (1983).
[11]W. C. Fon, K. A. Berrington, P. G. Burke, and A. E. Kingston, J. Phys. B **14**, 2921 (1981).
[12]S. W. Chiu and D. M. Schrader, Phys. Rev. A **33**, 2339 (1986).
[13]A. S. Ghosh and P. S. Grover, in *Positron Annihilation*, Proceedings of the Seventh International Conference on Positron Annihilation, New Delhi, 1985, edited by P. C. Jain, R. M. Singru, and K. P. Gopinathan (World Scientific, Singapore, 1986), p. 307.
[14]T. S. Stein and W. E. Kauppila, in *Electronic & Atomic Collisions: Invited Papers of the Fourteenth International Conference on the Physics of Electronic and Atomic Collisions, Palo Alto, CA, 1985*, edited by D. C. Lorents, W. E. Meyerhof, and J. R. Peterson (Elsevier, New York, 1986), p. 105.
[15]L. C. Green, M. M. Mulder, M. N. Lewis, and J. W. Woll, Phys. Rev. **93**, 757 (1954); F. W. Byron, Jr. and C. J. Joachain, *ibid.* **146**, 1 (1966).
[16]P. M. Morse, L. A. Young, and E. S. Haurwitz, Phys. Rev. **48**, 948 (1935).
[17]A. W. Weiss, J. Res. Nat. Bur. Stand. Sect. A **71**, 163 (1967).
[18]D. S. F. Crothers and R. P. McEachran, J. Phys. B **3**, 976 (1970).
[19]J. B. Furness and I. E. McCarthy, J. Phys. B **6**, 2280 (1973).
[20]R. Vanderpoorten, J. Phys. B **8**, 926 (1975).
[21]A. Temkin and J. C. Lamkin, Phys. Rev. **121**, 788 (1961).
[22]S. P. Khare and B. L. Moiseiwitsch, Proc. Phys. Soc. London **85**, 821 (1965).
[23]N. Onda and D. G. Truhlar, Phys. Rev. A **22**, 86 (1980).
[24]L. A. Parcell, R. P. McEachran, and A. D. Stauffer, J. Phys. B **16**, 4249 (1983); A. Dalgarno and N. Lynn, Proc. Phys. Soc. London, Sect. A **70**, 223 (1957).
[25]D. M. Schrader, Phys. Rev. **20**, 933 (1979).
[26]D. F. Register, S. Trajmar, and S. K. Srivastava, Phys. Rev. A **21**, 1134 (1980).
[27]W. R. Newell, D. F. C. Brewer, and A. C. H. Smith, J. Phys. B **14**, 3209 (1981).
[28]D. Andrick and A. Bitsch, J. Phys. B **8**, 393 (1975).
[29]T. Scott and H. S. Taylor, J. Phys. B **12**, 3385 (1979).
[30]R. W. LaBahn and J. Callaway, Phys. Rev. A **2**, 366 (1970).
[31]J. W. McConkey and J. Preston, J. Phys. B **8**, 63 (1975).
[32]S. K. Sethuraman, J. A. Rees, and J. R. Gibson, J. Phys. B **7**, 1741 (1974).
[33]R. H. Jansen, F. J. deHeer, H. J. Luyken, B. Van Wingerden, and H. J. Blaauw, J. Phys. B **9**, 185 (1976).
[34]F. W. Byron, Jr. and C. J. Joachain, J. Phys. B **10**, 207 (1977); Phys. Rev. A **15**, 128 (1977).
[35]R. K. Nesbet, Phys. Rev. A **20**, 58 (1979).
[36]H. J. Blaauw, R. W. Wagenaar, D. H. Barends, and F. J. deHeer, J. Phys. B **13**, 359 (1980).
[37]R. E. Kennerly and R. A. Bonham, Phys. Rev. A **17**, 1844 (1978).
[38]M. Charlton, T. C. Griffith, G. R. Heyland, and T. R. Twomey, J. Phys. B **13**, L239 (1980).
[39]F. J. deHeer and R. H. J. Jansen, J. Phys. B **10**, 3741 (1977).
[40]J. C. Nickel, K. Imre, D. F. Register, and S. Trajmar, J. Phys. B **18**, 125 (1985).
[41]T. Bhattacharya, Indian J. Phys. **35**, 623 (1961).
[42]I. R. Taylor, J. Phys. B **8**, 2810 (1975).
[43]S. T. Chen and G. A. Khayrallah, Phys. Rev. A **14**, 1639 (1976).
[44]R. Marriot, Proc. Phys. Soc. London **87**, 407 (1966).
[45]P. G. Burke, J. W. Cooper, and S. Ormonde, Phys. Rev. **183**, 245 (1969).
[46]R. C. Sklarew and J. Callaway, Phys. Rev. **175**, 103 (1968).
[47]R. S. Oberoi and R. K. Nesbet, Phys. Rev. A **8**, 2969 (1973).
[48]D. Hussain, A. D. Choudhary, A. K. Rafiqullah, C. W. Nestor, Jr., and F. B. Malik, Phys. Rev. **161**, 68 (1967).
[49]E. J. Robinson, Phys. Rev. **182**, 196 (1969).

[50]W. G. Wilson and W. L. Williams, J. Phys. B **9**, 423 (1976).
[51]R. H. Neynaber, S. M. Trujillo, L. L. Marino, and E. W. Roth, in *Proceedings of the Third International Conference on the Physics of Electronic and Atomic Collisions,* edited by M. McDowell (Wiley, New York, 1964), p. 1089.
[52]K. F. Canter, P. G. Coleman, T. C. Griffith, and R. G. Heyland, J. Phys. B **5**, L167 (1972); **6**, L201 (1973).
[53]T. S. Stein, W. E. Kaupilla, V. Pol, J. H. Smart, and G. Jesion, Phys. Rev. A **17**, 1600 (1973).
[54]P. G. Coleman, J. D. McNutt, L. M. Diana, and J. R. Burciaga, Phys. Rev. A **20**, 145 (1979).
[55]G. Sinapius, W. Raith, and W. G. Nilson, J. Phys. B **13**, 4079 (1980).
[56]T. Mizogawa, Y. Nakayama, T. Kawaratani, and M. Tosaki, Phys. Rev. A **31**, 2171 (1985).
[57]M. Ya. Amusia, N. A. Cherepkov, L. V. Chernysheva, and S. G. Shapiro, J. Phys. B **9**, L531 (1976).
[58]R. P. McEachran, D. L. Morgan, A. G. Ryman, and A. D. Stauffer, J. Phys. B **10**, 663 (1977).
[59]S. L. Willis, J. Hata, M. R. C. McDowell, C. J. Joachain, and F. W. Byron, Jr., J. Phys. B **14**, 2687 (1981).
[60]A. Mukherjee and D. P. Sural, J. Phys. B **15**, 1121 (1982).
[61]G. P. Gupta and K. C. Mathur, J. Phys. B **12**, 3071 (1979).
[62]Indira Khurana, Ph.D. thesis, University of Roorkee, 1987.